Air Quality, Atmosphere & Health (2019) 12:297–303
https://doi.org/10.1007/s11869-018-0653-6

Introduction of fractal-like agglomerates to the algorithm for calculating surface area concentrations of PM1

Dorota Bełkowska-Wołoczko[1]

Received: 10 June 2018 / Accepted: 20 November 2018 / Published online: 26 December 2018

Abstract
A method of estimating, in urban indoor environments, human exposure to particulate matter with aerodynamic diameter of less than 1 μm (PM1, also referred in the literature as fine-mode or nanometer (nm) particulate matter) is proposed. It defines a measure of exposure as a surface area concentration of PM1 and the means of its calculation. The calculation algorithm was constructed using statistical parameters of particulate matter lognormal distribution, with the use of Hatch-Choate equations and the Maynard method, and extended by the accumulation stage physics of PM1 fraction, including Eggersdorfer's and Pratsinis's findings. Introduction of structure and dynamics of fractal-like agglomerates into the calculation algorithm significantly increased estimation accuracy of surface area concentrations, in relation to the standard Maynard method, which calculates surface area concentrations of only spherical particles.

Keywords Air quality · Exposure assessment · Particulate matter · PM1 · Surface area concentration · Fractal-like agglomerates · Maynard method generalization

Introduction

Current air quality standards regarding particulate matter relate to mass concentrations of PM10 and PM2.5. Nevertheless, the importance of exposure to nanometer particulate matter (PM1) and its impact on health have been acknowledged in many research works (Chapman et al. 1997; Jones 1999; Pope III and Dockery 2006). The smaller the particles the larger their total surface area in relation to the total mass in a given air volume (Massey et al. 2012). In studies by Donaldson et al. (2001) and Oberdörster et al. (2005), a close relationship between the surface concentration of particles and organism's inflammatory response was noticed. Small-sized particulate matter may become a potential carrier of dangerous chemical compounds, which can easily penetrate to the end parts of airways and circulatory system (Ljungman 2009), and a site of possible adsorption of substances that may have allergenic and mutagenic effects (Pośniak et al. 2010). Furthermore, they can cause inflammation of the lungs, cardiovascular diseases, or even cancer (Donaldson et al. 2006). Polycyclic aromatic hydrocarbons (PAHs), which are mutagenic and carcinogenic substances, can be found in fine-mode particulate matter both in outdoor and indoor spaces (Błaszczyk et al. 2017). Traffic emissions can be a major source of nanometer particulate matter in urban air (Vu et al. 2018). High-transport intensity areas show that about 70–80% of toxic trace elements are contained within the PM1 fraction (Lin et al. 2005).

The discovery of health hazards that nanometer particulate matter may cause introduced a period of measurements of PM1 levels in atmospheric air and indoor spaces. However, due to lack of standards in this matter, PM1 fraction is studied from various aspects of its presence in the air, including measurements and estimations of mass, number and surface area concentrations, and chemical composition. Nevertheless, surface area concentration, which is related to reactivity and toxicity of nanometer (nm) particles may accurately reflect human exposure to PM1 pollution. The physics of typical urban air also supports the significance of surface area concentrations. Particles up to 100 nm which originate from emissions (e.g., during combustion processes) and arise as a result of homogeneous nucleation, otherwise described as condensation of supersaturated vapors (Jacobson 2002), dominate the number distribution of a typical urban aerosol (Morawska et al. 2004). In the accumulation mode, these nucleation particles grow and accumulate together by transformations, such as condensation and coagulation, into new structures (with

✉ Dorota Bełkowska-Wołoczko
dorotabelkowska@wp.pl

[1] Warsaw University of Technology, Warsaw, Poland

dimensions approximately from 100 nm to 1 μm). Accumulation mode structures dominate the surface area distribution of typical urban aerosol. Coarse particles, above 1 μm, are mainly formed in mechanical processes and they dominate the mass distribution of typical urban aerosol.

Accumulation mode products are complex structures; hence, Euclidean geometry is incapable of describing their shape effectively. They have been referred to as amorphous or filamentary. In the late twentieth century, computer technology and new fractal geometry concepts (Mandelbrot 1977, 1982) initiated experiments and numerical simulations of cluster structures of particles. These studies were carried out mainly as a result of a strong need to find an effective and unique method to describe aerosol particle characteristics and reflect their origin and physics. Experimental techniques used to investigate irregularly shaped structures included light scattering and transmission electron microscopy (TEM) (Lin et al. 1990; Puri et al. 1993; Wentzel et al. 2003). Researchers have found that atmospheric agglomerates (for, e.g., soot and fly ash) grow mainly by cluster–cluster coagulation and reveal self-similarity; hence, they can be called fractal-like structures that follow the rules of power law scaling (Lee et al. 2003; Zhu et al. 2005; Lushnikov et al. 2013). Thus, the introduction of fractal geometry enabled a convenient and effective mathematical description of structures like particulate matter agglomerates and provided a way to parameterize aerosol properties.

Measurements of PM1 concentrations in the air that directly surrounds humans are important for the accurate assessment of possible exposure. Measurements by portable apparatus, taken in real time, provide immediate results and continuous recording. Such measurements can follow human daily activity paths to reveal total and average PM1 levels for a given period in different environments, instantaneous changes and peaks when high pollution intensity occurs, and expose aerosol concentrations within indoor spaces where people tend to spend most of their time during the day (Vu et al. 2017). Currently, a majority of available apparatus for on-line measurements of surface area concentrations are stationary and use various assumptions to convert measured quantities, for example, converting electric charge to surface area. Thus, the calculation algorithm uses results from mass and number concentration measurements taken by widely accessible portable on-line apparatus. These light portable meters enable field measurements and aerosol particle collection from places where people live, work, and commute.

Methods

The calculation algorithm for establishing surface area concentration of PM1 is partially based on the standard Maynard method and partially uses a model of fractal-like agglomerates (Fig. 1). Such fractal-like agglomerates are common structures of, among others, soot particles in an accumulation mode (Shapiro et al. 2012).

The standard method for estimation of surface area concentration, developed by Maynard (2003), uses information from two independent and simultaneous measurements of mass and number concentrations. Unimodal, lognormal distribution of particles, and their spherical shape and fixed density are the basic assumptions of this method. However, surface area calculations that rely only on measured mass and number concentrations require determining the geometrical standard deviation σ. Maynard has noticed, while analyzing measurements of beryllium aerosol by McCawley et al. (2001), that the distributions of nanometer aerosol particles are characterized by standard deviation values in the range of 1.5 to 2, and that $\sigma = 1.8$ more accurately describes surface area distribution of the studied aerosol. This value was taken as one of the inputs into the calculation algorithm in the section where the Maynard method was adopted.

In the Maynard part of the calculations, to estimate surface area concentration, the count median diameter c needs to be established. It can be obtained by minimizing discrepancies (striving to 0) between the measured number N and mass M concentrations and the theoretical (expected) concentration values for the assumed lognormal distribution of aerosol particles. Therefore, c is derived by iterations for the lowest result of chi-square test (Maynard 2003). Hatch-Choate equations (Hatch and Choate 1929) describe properties of the lognormal particle size distribution. From the relationships described there, between geometric standard deviation σ and count median diameter c, it is possible to calculate the diameter d_s for the average surface area:

$$d_s = c \times e^{ln^2 \sigma} \quad (1)$$

Hence, with the measured number concentration N, surface area concentration SA_M of spherical particles in the studied aerosol can be derived with the use of the Maynard method:

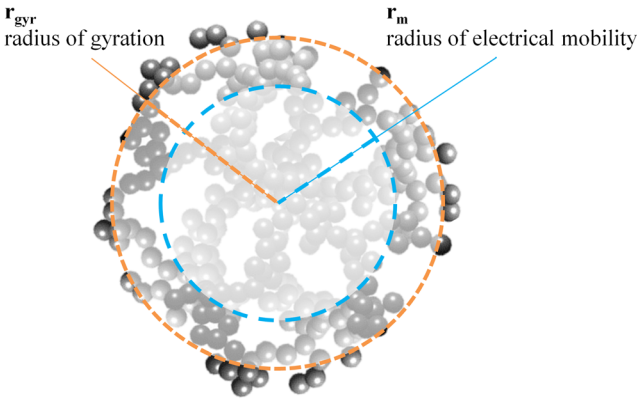

Fig. 1 Agglomerate model with its characteristic radius metrics (Bełkowska-Wołoczko 2017)

$$SA_M = N \times \pi \times d_s^2 \tag{2}$$

The model of a fractal-like agglomerate is an idealistic form that serves as a foundation for the design of the calculation algorithm. To construct this model, the nature of forming structures in accumulation mode and dependencies from the particle physics domain were used. The additional assumption was made that the agglomerate model consists of identical spherical primary particles with diameter d_{pp} (monodisperse). The spatial structure of the agglomerate model can be specified by the arrangement of primary particles in relation to the center of its mass. The radius of gyration r_{gyr} represents this measure—mean square distance from the furthest points to the center of gravity of the agglomerate (Philippe 2017). The diameter of the electrical mobility of agglomerate d_m is equal to the diameter of the sphere, which is characterized by an identical trajectory in the electric field (Rissler et al. 2013). Hence, the radius of electrical mobility $r_m = \frac{dm}{2}$.

The calculation algorithm assumes that the number of identical agglomerate models is equal to the number of all individual particles and their clusters occurring in the tested aerosol. With this assumption, the mass of the agglomerate model m_{agg} can be averaged from the total measured mass concentration M divided by the measured number concentration N of all structures:

$$m_{agg} = N_{pp} \times m_{pp} = \frac{M}{N} \tag{3}$$

As all agglomerate models are identical, as well as the mass of primary particles m_{pp}, their number can be derived from the above equation (Eq. 3):

$$N_{pp} = \frac{M}{N \times m_{pp}} \tag{4}$$

The mass of monodisperse primary particles in the agglomerate model is equal to:

$$m_{pp} = \frac{\rho_{pp} \times \pi \times d_{pp}^3}{6} \tag{5}$$

where density of primary particles ρ_{pp} was assumed at 2100 kg·m^{-3} (density of soot particles, particles emitted by diesel engines, measured by pycnometric method (Hougaard et al. 2008)) and diameter d_{pp} of primary particles is constant and amounts to 15 nm. This last value corresponds to high numerical concentrations of the urban aerosol at the nucleation mode (Morawska et al. 2004). From these individual particles, agglomerates at the accumulation mode are created.

The number of monodisperse primary particles N_{pp}, all with radius r_{pp}, and radius of gyration r_{gyr} of the agglomerate model are related with each other in the power functions describing the nature of fractals (Matsoukas and Friedlander 1991):

$$N_{pp} = k \times \left(\frac{r_{gyr}}{r_{pp}}\right)^{D_f} \tag{6}$$

where, D_f is a fractal dimension and k is a factor associated with D_f.

The formation of agglomerates is a phenomenon resulting directly from physical movements of particles in the air. Both constants D_f and k depend on the mechanism of formation of fractal-like agglomerates, spatial distribution of primary particles, and their diversity (mono- or polydisperse). Products of agglomeration processes have a fractal dimension D_f that is usually in the range of 1.3–3.0 (from fractal-like structures to ideal sphere) and $k \approx 0.4$–3.5 (Lushnikov 2010; Eggersdorfer and Pratsinis 2012). Agglomerates with a lower D_f have a more open structure and dendritic shape with larger collision cross sections but lower mobility. Conversely, agglomerates which present compact, dense structures up to a spherical shape reached for $D_f = 3$. Thus, it can be concluded that the spatial distribution of primary particles in the agglomerate affects its kinetic properties.

It is assumed that the most important mechanism responsible for the coagulation of nanometer particles in the air is Brownian diffusion (Otto and Fissan 1999; Chen 2012), as a collective average behavior of all particles. Forms constructed in this way resemble diffusion-limited cluster–cluster agglomerates (DLCA) (Eggersdorfer and Pratsinis 2014). For this DLCA formation mechanism, with the Knudsen diffusion number $K_n \approx 0.1$–1, and an assumption of monodisperse primary particles, fractal-related constants were determined: the mass fractal dimension $D_f = 1.8$, which reflects the complexity of the agglomerate, and the coefficient describing the mechanism of the collision of primary particles forming agglomerates $k = 1.3$.

The surface area concentration of all primary particles SA_{pp} in the studied aerosol can be derived with the use of results of number concentration measurements N, which describe the number of fractal-like agglomerate models in the studied aerosol, and the data on the diameter of spherical primary particles d_{pp}, and their number N_{pp} in one cluster:

$$SA_{pp} = N \times N_{pp} \times \pi \times d_{pp}^2 \tag{7}$$

The calculation algorithm determines the shape of the agglomerate models by the introduced coefficient of spatial mass distribution g. Its values depend on the agglomerate's spatial arrangement of primary particles, described by the radius of gyration r_{gyr}, and their number N_{pp}, at a given radius $r_{pp} = \frac{d_{pp}}{2}$. The radius of gyration of agglomerate model can be then determined by combining Eq. 6 with Eq. 4 and Eq. 5:

$$r_{gyr} = r_{pp} \times \left(\frac{6 \times M}{\rho_{pp} \times \pi \times d_{pp}^3 \times k \times N}\right)^{\frac{1}{D_f}} \tag{8}$$

Therefore, with known r_{gyr}, N_{pp}, and r_{pp}, the coefficient of spatial mass distribution g is also known:

$$g = \frac{r_{gyr}}{\left(N_{pp} \times r_{pp}\right)} \tag{9}$$

Calculations of surface area concentration of structures with the lower number of primary particles SA_1, up to approx. 5000, are based on the fractal-like agglomerate model and its ability to fill the space and the Maynard method. Therefore, if the agglomerate model adopts a more open structure with a larger radius of gyration, then more primary particles are accessible for interactions at their surface and the coefficient g strengthens. Conversely, when primary particles are more densely packed and the structure resembles a sphere, then the standard Maynard method for calculating surface area of spherical particles becomes dominant. These assumptions are revealed in the below equation which is a merger of Eq. 2, Eq. 7, and Eq. 9:

$$SA_1 = SA_{pp} \times g + SA_M \times (1-g) \tag{10}$$

For agglomerates with the number of primary particles N_{pp} above approx. 5000, surface area concentration SA_2 is calculated with the use of mobility theory. The diameter of electric mobility d_m is characteristic and one of the basic measures of agglomerates. For the DLCA formation mechanism, mobility diameter d_m is proportional to the primary particles' diameter d_{pp} (Rissler et al. 2013):

$$d_m = d_{pp} \times \left(10^{-2\times 0.51+0.92}\right) \times N_{pp}^{0.51} \tag{11}$$

Therefore, the mobility-based surface area concentration SA_2 can be derived from the equation reflecting projected surface area (Rogak et al. 1993) of the agglomerate model, measured number concentration N, and agglomerate mobility diameter d_m:

$$SA_2 = N \times \pi \times \frac{d_m^2}{4} \tag{12}$$

Depending on the calculated number of primary particles N_{pp} in the agglomerate model, the algorithm selects the formula SA_1 (Eq. 10) or SA_2 (Eq. 12) from which the surface area concentration of PM1 is calculated. This division was determined from calculations of the surface area for one agglomerate model based on relationships between characteristic radius metrics of this structure, as described in Eggersdorfer and Pratsinis (2014) work for different quantities of primary particles. It was noticed that calculations of SA_1 based on the fractal-like concept complemented with the Maynard method provide incoherent results for agglomerates with more than approx. 5000 primary particles. It may be explained by the nature of the accumulation process, where particles first coagulate creating simple structures and then grow further into complex agglomerates. The sizes of primary particles are less than the mean free path of molecules (68 nm), while the sizes of the agglomerates may far exceed them. The kinetics of these structures change during this process. The probability that the small particles in the collision will rebound from each other is small, mainly due to their low kinetic energy, while for complex and dense clusters their mobility starts to be a significant characteristic. The electrical mobility is directly related to the quantity of electric charge applied to the accessible surface area of the structure (Ku 2010); thus, it may describe complex agglomerates with several, or even tens of thousands of primary particles, in a more accurate way. Therefore, it was adopted that for clusters with primary particles number N_{pp} exceeding approx. 5000, surface area concentration SA_2 can be calculated based on electrical mobility diameter d_m of an agglomerate model.

Results and discussion

The calculation algorithm was verified with the use of data from 7 different studies (Park et al. 2009, 2010; Buonanno et al. 2010; Ham et al. 2012; Jankowska and Pośniak 2012; Castro et al. 2015; Spinazzè et al. 2015) in which 3 concentrations of particulate matter, mass M [commonly used unit $\mu g \cdot m^{-3}$], number N [commonly used unit cm^{-3}], and surface area SA [commonly used unit $\mu m^2 \cdot m^{-3}$], were measured simultaneously. Measured concentrations of M and N were used as inputs for both the calculation algorithm and the standard Maynard method to estimate SA concentrations. Results of SA concentrations were compared between measured and estimated by the calculation algorithm, and between measured and calculated by the standard Maynard method for spherical particles.

Sensitivity of the calculation algorithm is presented in Table 1, where different input assumptions for an agglomerate model were tested. The highest coefficient of determination (R^2) can be noticed for primary particles' diameter d_{pp} = 15 nm, D_f = 1.8, and k = 1.3. For these parameters, statistical analysis revealed a very strong correlation between the surface area concentrations measured and estimated by the calculation algorithm (Pearson correlation coefficient r = 0.852), significantly higher than that in the case of the standard Maynard method (r = 0.740). In addition, the Maynard method showed a statistically significant difference between measured and calculated surface area concentrations in paired t test. Conversely, in the case of the calculation algorithm, this relationship could not be ruled out. The mean squared error (MSE) of the difference between the measured and estimated surface area concentration was significantly lower in the case of the calculation algorithm (MSE = 0.09) than that in the case of the standard Maynard method (MSE = 0.41).

Table 1 Calculation algorithm sensitivity with R^2 and %ΔSA (difference between estimated and measured surface area concentration) for different agglomerate model types

Structure type	Fractal dimension	Primary particle diameter		
		d_{pp} = 10 nm	d_{pp} = 15 nm	d_{pp} = 20 nm
Fractal-like agglomerate chain type	Df = 1	%ΔS = 111%	%ΔS = 91%	%ΔS = 49%
	k = 3.5	R^2 = 0.83	R^2 = 0.84	R^2 = 0.84
Fractal-like agglomerate open type	Df = 1.8	%ΔS = 75%	%ΔS = 15%	%ΔS = 11%
	k = 1.3	R^2 = 0.86	R^2 = 0.91	R^2 = 0.86
Fractal-like agglomerate dense type	Df = 2.8	%ΔS = 8%	%ΔS = − 24%	%ΔS = − 27%
	k = 1.1	R^2 = 0.87	R^2 = 0.90	R^2 = 0.88
Individual spherical particles	Df = 3	%ΔS = − 16%	%ΔS = − 35%	%ΔS = − 32%
	k = 1	R^2 = 0.73	R^2 = 0.79	R^2 = 0.78
Individual spherical particles	Maynard	%ΔS = − 40%; R^2 = 0.80		

The relationship between measured (literature data) and estimated (by the standard Maynard method and by the calculation algorithm) surface area concentrations (precisely their logarithms) is visualized in Fig. 2.

For all seven studies, slightly over 70% of all calculations were based on SA_1 for $N_{pp} < 5000$, and the rest referred to SA_2, which was estimated on the basis of electrical mobility theory. In calculations of SA_1, the g coefficient varied between 3 and 20%. This means that the algorithm accounts for up to 20% of the calculated surface area of every primary particle in the agglomerate models and complements it with Maynard's calculations for spherical particles. Consequently, results of this study are in line with earlier findings (Ku and Evans 2012; Wierzbicka et al. 2014) suggesting that the surface area concentrations calculated with the standard Maynard method itself might have been underestimated, by as much as 40%, due to the fact that this method does not include structures formed in an accumulation mode.

Conclusions

Information on PM1 mass, number, and surface area concentration levels creates a multidimensional description of exposure to nanometer particulate matter in the urban environment. Surface area concentrations can be applied as the main exposure indicator for PM1, containing baseline information on the reactivity of particulate matter. Data on number concentrations supplement this information with the data on intensity of sources, whereas results of mass concentrations measurements can be used to compare them with PM2.5 air quality standards as the nearest reference.

Due to the generalization of the standard Maynard method to the nucleation and accumulation modes, and the significance of the results of statistical analysis, the calculation algorithm could be used to estimate surface area concentrations of PM1 based on simultaneous mass and number concentration measurements. Further measurements and comparisons are

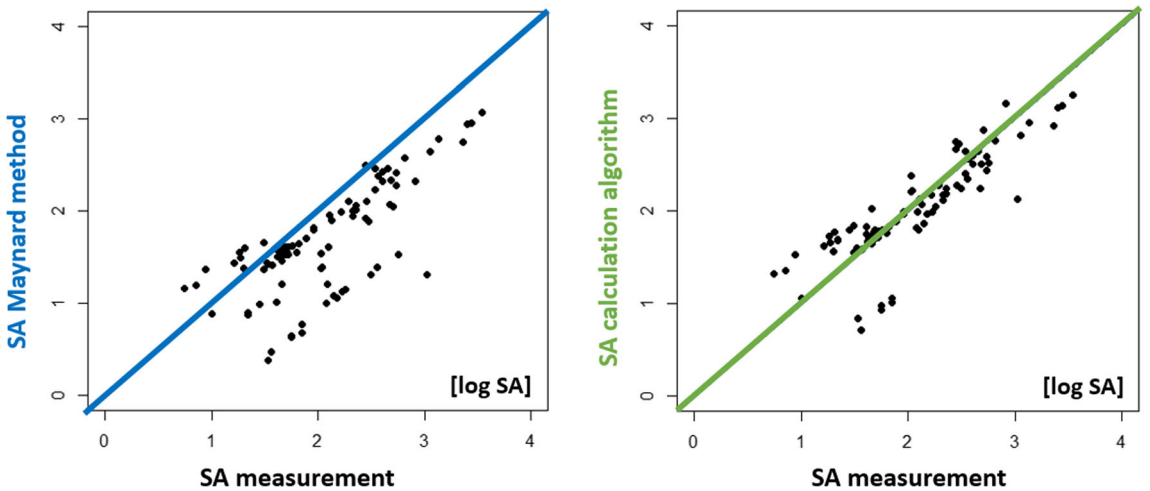

Fig. 2 Correlation of surface area concentrations measured and estimated by the standard Maynard method (*left*) and the calculation algorithm based on the agglomerate model (*right*) (Bełkowska-Wołoczko 2017). Values are log-transformed

needed to strengthen this statement. Additional generalizations, e.g., onto polydisperse primary particles, could enhance the accuracy of the calculation algorithm.

References

Bełkowska-Wołoczko D (2017) Stężenia powierzchniowe jako wskaźnik ekspozycji człowieka na submikronowe cząstki pyłów zawieszonych. PhD dissertation, Warsaw University of Technology, Warsaw, Poland

Błaszczyk E, Rogula-Kozłowska W, Klejnowski K, Fulara I, Mielżyńska-Švach D (2017) Polycyclic aromatic hydrocarbons bound to outdoor and indoor airborne particles (PM2.5) and their mutagenicity and carcinogenicity in Silesian kindergartens, Poland. Air Qual Atmos Health 10:389–400. https://doi.org/10.1007/s11869-016-0457-5

Buonanno G, Morawska L, Stabile L, Viola A (2010) Exposure to particle number, surface area and PM concentrations in pizzerias. Atmos Environ 44:3963–3969. https://doi.org/10.1016/j.atmosenv.2010.07.002

Castro A, Calvo AI, Alves C, Alonso-Blanco E, Coz E, Marques L, Nunes T, Fernández-Guisuraga JM, Fraile R (2015) Indoor aerosol size distributions in a gymnasium. Sci Total Environ 524:178–186. https://doi.org/10.1016/j.scitotenv.2015.03.118

Chapman RS, Watkinson WP, Dreher KL, Costa DL (1997) Ambient particulate matter and respiratory and cardiovascular illness in adults: particle-borne transition metals and the heart–lung axis. Environ Toxicol Pharmacol 4:331–338

Chen Z-L (2012) Brownian coagulation of aerosols in transition regime. Therm Sci 16(5):1362–1366. https://doi.org/10.2298/TSCI1205362C

Donaldson K, Stone V, Clouter A, Renwick L, MacNee W (2001) Ultrafine particles. Occup Environ Med 58(3):211–216

Donaldson K, Aitken R, Tran L, Stone V, Duffin R, Forrest G, Alexander A (2006) Carbon nanotubes: a review of their properties in relation to pulmonary toxicology and workplace safety. Toxicol Sci 92(1):5–22. https://doi.org/10.1093/toxsci/kfj130

Eggersdorfer ML, Pratsinis SE (2012) The structure of agglomerates consisting of polydisperse particles. Aerosol Sci Technol 46(3):347–353. https://doi.org/10.1080/02786826.2011.631956

Eggersdorfer ML, Pratsinis SE (2014) Agglomerates and aggregates of nanoparticles made in the gas phase. Adv Powder Technol 25:71–90. https://doi.org/10.1016/j.apt.2013.10.010

Ham S, Yoon C, Lee E, Lee K, Park D, Chung E, Kim P, Lee B (2012) Task-based exposure assessment of nanoparticles in the workplace. J Nanopart Res 14(1126):1–17. https://doi.org/10.1007/s11051-012-1126-8

Hatch T, Choate SP (1929) Statistical description of the size properties of non uniform particulate substances. J Frankl Inst 207(3):369–387. https://doi.org/10.1016/S0016-0032(29)91451-4

Hougaard KS, Jensen KA, Nordly P, Taxvig C, Vogel U, Saber AT, Wallin H (2008) Effects of prenatal exposure to diesel exhaust particles on postnatal development, behavior, genotoxicity and inflammation in mice. Part Fibre Toxicol 5(3):1–15. https://doi.org/10.1186/1743-8977-5-3

Jacobson MZ (2002) Atmospheric pollution: history, science, and regulation. Cambridge University Press, Cambridge, p 399 ISBNs 0 521 01044 6, 0 521 81171 6

Jankowska E, Pośniak M (2012) Aerozole emitowane w procesach wysokotemperaturowych - wytyczne do oceny narażenia zawodowego. CIOP-PIB, Warsaw ISBN 978-83-7373-115-8

Jones AP (1999) Indoor air quality and health. Atmos Environ 33(28):4535–4564. https://doi.org/10.1016/S1352-2310(99)00272-1

Ku BK (2010) Determination of the ratio of diffusion charging-based surface area to geometric surface area for spherical particles in the size range of 100–900 nm. J Aerosol Sci 41(9):835–847. https://doi.org/10.1016/j.jaerosci.2010.05.008

Ku BK, Evans DE (2012) Investigation of aerosol surface area estimation from number and mass concentration measurements. Aerosol Sci Technol 46(4):473–484. https://doi.org/10.1080/02786826.2011.639316

Lee KO, Zhu J, Ciatti S, Yozgatligil A, Choi MY (2003) Sizes, graphitic structures and fractal geometry of light-duty diesel engine particulates. SAE Technical Paper 2003-01-3169, pp 12. https://doi.org/10.4271/2003-01-3169

Lin MY, Klein R, Lindsay ML, Weitz DA, Ball RC, Maekin P (1990) The structure of fractal colloidal aggregates of finite extent. J Colloid Interface Sci 137(1):263–280. https://doi.org/10.1016/0021-9797(90)90061-R

Lin CC, Chen SJ, Huang KL, Hwang WI, Chang-Chien GP, Lin WY (2005) Characteristics of metals in nano/ultrafine/fine/ coarse particles collected beside a heavily trafficked road. Environ Sci Technol 39(21):8113–8122. https://doi.org/10.1021/es048182a

Ljungman P (2009) Cardiovascular effects of short-term exposure to air pollution: exploring potential pathways and susceptible subgroups. PhD dissertation, Karolinska Institutet, Stockholm, Sweden. ISBN: 978-91-7409-454-1

Lushnikov AA (2010) Introduction to aerosols. In: Agranovski I (ed) Aerosols—science and technology. WILEY-VCH Verlag GmbH & Co. KGaA, Weinheim, p 42 ISBN: 978-3-527-32660-0

Lushnikov AA, Gvishiani AD, Lyubovtseva YS (2013) Fractal aggregates in the atmosphere. Russ J Earth Sci 13(ES2003):1–7. https://doi.org/10.2205/2013ES000531

Mandelbrot BB (1977) Fractals: form, chance, and dimension. W H Freeman and Company Ltd, San Francisco, p 365 ISBN-10: 0716704730, ISBN-13: 978-0716704737

Mandelbrot BB (1982) The fractal geometry of nature. W H Freeman and Company Ltd, San Francisco, p 480 ISBN-10: 9780716711865, ISBN-13: 978–0716711865

Massey D, Kulshrestha A, Masih J, Taneja A (2012) Seasonal trends of PM10, PM5.0, PM2.5 & PM1.0 in indoor and outdoor environments of residential homes located in north-central India. Build Environ 47:223–231. https://doi.org/10.1016/j.buildenv.2011.07.018

Matsoukas T, Friedlander SK (1991) Dynamics of aerosol agglomerate formation. J Colloid Interface Sci 146(2):495–506. https://doi.org/10.1016/0021-9797(91)90213-R

Maynard AD (2003) Estimating aerosol surface area from number and mass concentration measurements. Ann Occup Hyg 47(2):123–144. https://doi.org/10.1093/annhyg/meg022

McCawley MA, Kent MS, Berakis MT (2001) Ultrafine beryllium aerosol as a possible metric for chronic beryllium disease risk. Appl Occup Environ Hyg 16(5):631–638. https://doi.org/10.1080/10473220120812

Morawska L, Moore MR, Rostovski Z (2004) Health impacts of ultrafine particles, Canberra Act 2601: Commonwealth of Australia. Australian Department of the Environment and Heritage, Canberra ISBN 0642550557

Oberdörster G, Maynard A, Donaldson K, Castranova V, Fitzpatrick J, Ausman K, Carter J, Karn B, Kreyling W, Lai D, Olin S, Monteiro-Riviere N, Warheit D, Yang H (2005) Principles for characterizing the potential human health effects from exposure to nanomaterials: elements of a screening strategy. Part Fibre Toxicol 2:8. https://doi.org/10.1186/1743-8977-2-8

Otto E, Fissan H (1999) Brownian coagulation of submicron particles. Adv Powder Technol 10:1–20. https://doi.org/10.1016/S0921-8831(08)60453-7

Park JY, Raynor PC, Maynard AD, Eberly LE, Ramachandran G (2009) Comparison of two estimation methods for surface area concentration using number concentration and mass concentration of combustion related ultrafine particles. Atmos Environ 43(3):502–509. https://doi.org/10.1016/j.atmosenv.2008.10.020

Park JY, Ramachandran G, Raynor PC, Eberly LE, Olson G Jr (2010) Comparing exposure zones by different exposure metrics using statistical parameters: contrast and precision. Ann Occup Hyg 54(7):799–812. https://doi.org/10.1093/annhyg/meq043

Philippe A (2017) Evaluation of currently available techniques for studying colloids in environmental media: introduction to environmental nanometrology. In: Joo SH (ed) Applying nanotechnology for environmental sustainability. IGI Global, Hershey, PA, pp 1–26 ISBN: 9781522505853

Pope CA III, Dockery DW (2006) Health effects of fine particulate air pollution: lines that connect. J Air Waste Manage Assoc 56(6):709–742. https://doi.org/10.1080/10473289.2006.10464485

Pośniak M, Jankowska E, Szewczyńska M, Zapór L, Brochocka A, Pietrowski P (2010) Zagrożenia spalinami silników Diesla. CIOP-PIB, Warsaw ISBN: 978-83-7373-081-6

Puri R, Richardson TF, Santoro RJ, Dobbins RA (1993) Aerosol dynamic processes of soot aggregates in a laminar ethene diffusion flame. Combust Flame 92(3):320–333. https://doi.org/10.1016/0010-2180(93)90043-3

Rissler J, Messing ME, Malik AI, Nilsson PT, Nordin EZ, Bohgard M, Sanati M, Pagels JH (2013) Effective density characterization of soot agglomerates from various sources and comparison to aggregation theory. Aerosol Sci Technol 47(7):792–805. https://doi.org/10.1080/02786826.2013.791381

Rogak SN, Flagan RC, Nguyen HV (1993) The mobility and structure of aerosol agglomerates. Aerosol Sci Technol 18:25–47. https://doi.org/10.1080/02786829308959582

Shapiro M, Vainshtein P, Dutcher D, Emery M, Stolzenburg M, Kittelson DB, McMurry PH (2012) Characterization of agglomerates by simultaneous measurement of mobility, vacuum aerodynamic diameter and mass. J Aerosol Sci 44:24–45. https://doi.org/10.1016/j.jaerosci.2011.08.004

Spinazzè A, Cattaneo A, Scocca DR, Bonzini M, Cavallo DM (2015) Multi-metric measurement of personal exposure to ultrafine particles in selected urban microenvironments. Atmos Environ 110:8–17. https://doi.org/10.1016/j.atmosenv.2015.03.034

Vu TV, Ondracek J, Zdímal V, Schwarz J, Delgado-Saborit JM, Harrison RM (2017) Physical properties and lung deposition of particles emitted from five major indoor sources. Air Qual Atmos Health 10:1–14. https://doi.org/10.1007/s11869-016-0424-1

Vu TV, Zauli-Sajani S, Poluzzi V, Harrison RM (2018) Factors controlling the lung dose of road traffic-generated sub-micrometre aerosols from outdoor to indoor environments. Air Qual Atmos Health 11:615–625. https://doi.org/10.1007/s11869-018-0568-2

Wentzel M, Gorzawski H, Naumann K-H, Saathoff H, Weinbruch S (2003) Transmission electron microscopical and aerosol dynamical characterization of soot aerosols. J Aerosol Sci 34(10):1347–1370. https://doi.org/10.1016/S0021-8502(03)00360-4

Wierzbicka A, Nilsson PT, Rissler J, Sallsten G, Xu Y, Pagels JH, Albin M, Österberg K, Strandberg B, Eriksson A, Bohgard M, Bergemalm-Rynell K, Gudmundsson A (2014) Detailed diesel exhaust characteristics including particle surface area. Atmos Environ 86:212–219. https://doi.org/10.1016/j.atmosenv.2013.11.025

Zhu J, Lee KO, Yozgatligil A, Choi MY (2005) Effects of engine operating conditions on morphology, microstructure, and fractal geometry of light-duty diesel engine particulates. Proc Combust Inst 30(2):2781–2789. https://doi.org/10.1016/j.proci.2004.08.232